Article citation info:
Kuchmacz K, Noga M. 1D simulation of the impact of direct water injection on a small SI engine performance and emissions. Combustion Engines. 2025;200(1):105-116. https://doi.org/10.19206/CE-200067

Konrad KUCHMACZ
Marcin NOGA

Combustion Engines
Polish Scientific Society of Combustion Engines

1D simulation of the impact of direct water injection on a small SI engine performance and emissions

ARTICLE INFO

Received: 24 July 2024
Revised: 6 January 2025
Accepted: 13 January 2025
Available online: 14 February 2025

The paper contains results of a 1D simulation of the direct water injection for the four-stroke single-cylinder gasoline engine and shows a comparison between cycles with and without water addition. Various water injection timing, as well as water-to-fuel ratios, were considered, including injection during the compression stroke and just after finishing the combustion. Results show that direct water injection in internal combustion engines has a minimal effect on overall performance parameters but improves emission levels, particularly by reducing NO_x emissions. Injection at 100 deg bTDC consistently shows the greatest reduction in NO_x emissions across scenarios. However, late water injection during combustion increases HC emissions.

Key words: *spark ignition, direct water injection, low emissions, mechanical engineering, 1D simulation*

1. Introduction

The increasingly stringent emission standards for internal combustion engines and the global trend towards reducing CO_2 emissions have led engineers and scientists specializing in internal combustion engines to seek solutions to improve engine performance and reduce fuel consumption and emissions [11, 12]. One of the methods that allow for effectively reducing emissions, especially HC [5], NO_x [6], CO, and CO_2 [14], is water injection. Water, due to its properties, is an excellent cooling medium. Its high heat of vaporization of 2257 kJ/kg·K and large specific heat of 4200 kJ/kg·K allow water to be used to lower the average temperature of the engine cycle, thereby mitigating tendencies towards knock combustion, which enables the engine to operate more efficiently under high loads and also reduces emissions. The method of delivering water can be divided into two main methods: indirect injection [1, 4, 6, 8, 14] and direct injection [2, 3]. The overall engine parameters with water injection depend on the mass of injected water, water temperature, water-to-fuel mass ratio (W/F), and the timing of water injection. Lower values of W/F improve Brake Specific Fuel Consumption (BSFC), but an increase in the mass of injected water worsens it [7]. Proper injection timing, temperature, and mass, especially with the injection of superheated water, can improve engine performance metrics such as thermal efficiency and reduce engine thermal loads [2]. Water injection into a spark-ignition (SI) [7, 8] engine mitigates the knocking effect during high-load operation by reducing the temperature of the working fluid, this allows for more optimal fuel metering and ignition timing settings at high engine loads, ultimately resulting in better engine performance. The solution with indirect water injection into the intake manifold at high engine loads and speeds was implemented by BMW [17] in the BMW M4 GTS, equipped with the S55 engine. According to the manufacturer, this increased the engine's maximum power and torque without raising CO_2 emissions compared to the engine without additional water injection. However, the mass of water delivered to the cylinder must be precisely metered; an excessive water addition, due to incomplete evaporation, can result in dilution of the engine oil by the unevaporated water, leading to premature failures and decreased engine reliability [4, 14].

Recent studies on water injection in internal combustion engines include, among others: research on: counteracting the negative effects of water injection on the stability of the combustion process by using additional hydrogen injection [15], CFD analysis of water injection application in HCCI combustion system [9] and evaluation of the effect of water injection in a DISI engine fueled with gasoline with different percentages of ethanol [13].

The article compared the simulation results of engine operation with and without direct water injection. The subject of the simulation studies was a single-cylinder Honda GX160 engine with parameters listed in Table 1. This engine is air-cooled and equipped with a carburetor fuel supply system and fixed ignition timing for all engine operating conditions.

Table 1. Technical specifications of the Honda GX 160 engine

Engine type	Single cylinder, four stroke, spark ignition
Displacement	163 cm^3
Cylinder bore × stroke	68 × 45 mm
Connecting rod length	84 mm
Compression ratio	8.5:1
Rated power	3.6 kW
Maximum torque	10.3 Nm
Cooling system	Forced air-cooling
Ignition angle	27° bTDC
Fuel delivery system	Carburetor

The simulations were conducted using a 1D computational environment called GT Power. GT Power is a widely used program for one-dimensional simulations in the automotive industry and internal combustion engine sector. GT Power is used to predict engine parameters such as power, torque, air flow, volumetric efficiency, specific fuel consumption, and many other aspects related to the operation of internal combustion engines.

2. Numerical Model

The simulations covered the full engine operating cycle, including cylinder charge exchange. The computational schematic is shown in Fig. 1. The calibration parameters of the model, described in detail in the subsection, were obtained through evolutionary optimization with respect to in-cylinder pressure waveforms recorded during tests on the Honda GX160 engine [10].

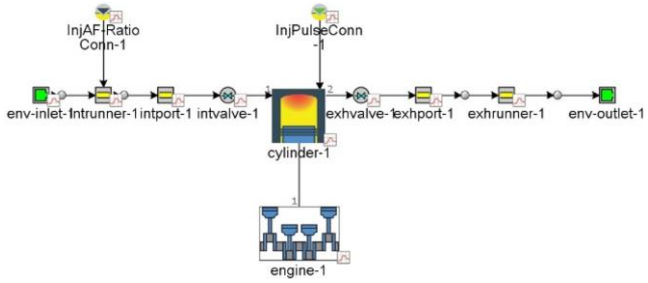

Fig. 1. Honda GX 160 engine model representation in GT Power environment

2.1. Flow modeling in GT Power

The flow model involves solving the Navier-Stokes equations, which consist of the continuity equation, momentum equations, and energy equation. These equations are solved in one dimension, meaning that all quantities are averaged in the flow direction. There are two possible time integration methods, which affect solution variables and time step constraints. Time integration methods include explicit and implicit integrators. The primary solution variables in the explicit method are mass flow, density, and internal energy, while in the implicit method, they are mass flow, pressure, and total enthalpy. Further details regarding each of these methods will be discussed below. The entire system is discretized into multiple volumes – Fig. 2, where each flow division is represented by a single volume, and each pipe is divided into one or more volumes. These volumes are connected by boundaries. It is assumed that scalar variables (pressure, temperature, density, internal energy, enthalpy, substance concentrations, etc.) are uniform in each volume. Vector variables (mass flow rate, velocity, mass fraction fluxes, etc.) are calculated for each boundary. This type of discretization is called a "staircase grid".

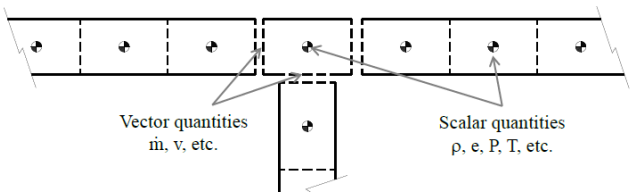

Fig. 2. The schematic of the staircase grid used for solving the Navier-Stokes equations in GT Power [16]

The applied equations have the following forms:

1. Continuity Equation:

$$\frac{dm}{dt} = \dot{m} \tag{1}$$

2. Energy Equation:

$$\frac{d(me)}{dt} = -\rho\frac{dV}{dt} + \sum(\dot{m}H) - hA_S(T_{fluid} - T_{wall}) \tag{2}$$

3. Momentum Equation:

$$\frac{d\dot{m}}{dt} = (dPA + \sum(\dot{m}u) - 4C_f\frac{\rho u|u|}{2}\frac{dxA}{D} - \\ -K_p\left(\frac{1}{2}\rho u|u|\right)A)\frac{1}{dx} \tag{3}$$

2.2. Charge exchange

For the modeled engine, the flow through the intake and exhaust valves was simulated according to the following equation:

$$m = A_{eff}\rho_{is}U_{is}^{\cdot} = C_D A_R \rho_{is} U_{is} \tag{4}$$

where:

$$\rho_{is} = \rho_o(P_R)^{\frac{1}{\gamma}} \tag{5}$$

$$U_{is} = \sqrt{RT_o}\left[\frac{2}{\gamma-1}(1 - P_R^{\frac{\gamma-1}{\gamma}})\right]^{\frac{1}{2}} \tag{6}$$

The flow cross-section area for the valves is a function of valve lift as a function of crankshaft rotation angle. The timing diagrams for the intake and exhaust valves for the considered Honda GX 160 engine are shown in a Fig. 3.

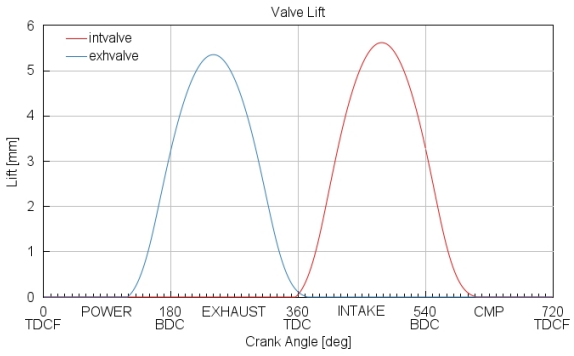

Fig. 3. The valve timing diagrams of the Honda GX 160 engine used for simulating the charge exchange process

For the valve type connection in the GT Power program, the flow resistance coefficient CD is a function of the lift-to-diameter ratio L/D of the valve. The CD coefficient used in the simulation for the intake and exhaust valve flows are presented in Fig. 4 and Fig. 5, respectively.

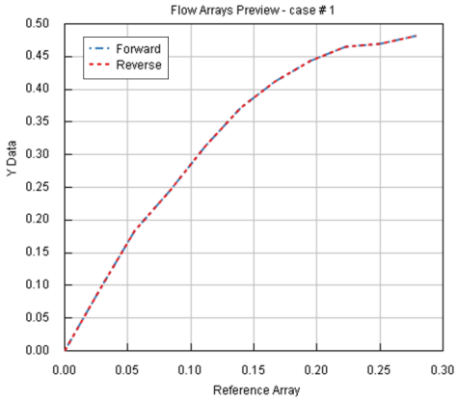

Fig. 4. The flow resistance coefficient CD vs L/D for the intake valve

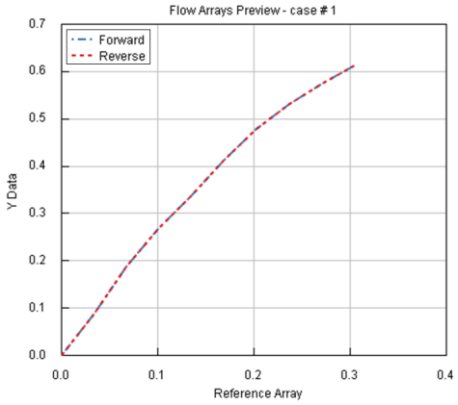

Fig. 5. The flow resistance coefficient CD vs L/D for the exhaust valve

2.3. Combustion model

In the simulation, the SITurb combustion model developed by GT Power was used for calculating combustion processes in spark ignition (SI) engines with a homogeneous fuel-air mixture. In GT Power's terminology, this model is referred to as the Predictive Combustion Model because it predicts the combustion rate considering air movement inside the cylinder, fuel properties, spark plug location, and combustion chamber geometries in either detailed or simplified form. This model is the only one in GT Power capable of estimating emission levels for SI engines. Based on four equation multipliers, calculations of the combustion process can be calibrated based on the measured actual indicated pressure of the engine. In the model, the combustion rate is proportional to the sum of laminar and turbulent flame velocities and the difference between the mass of burned products and fresh mixture ahead of the flame front divided by the time constant. The cylinder flow is described using a one-dimensional k-ε turbulence model, which calculates the required length scales and time scales for the SITurb model – eq. (7)–(14).

$$\frac{dM_b}{dt} = \frac{(M_e - M_b)}{\tau} \tag{7}$$

$$\frac{dM_e}{dt} = \rho_u A_e (s_T + s_L) \tag{8}$$

$$\tau = \frac{\lambda}{S_L} \tag{9}$$

$$\lambda = \frac{C_{TlS} L_i}{\sqrt{Re}} \tag{10}$$

$$Re = \frac{\rho_u u' L_i}{\mu_u} \tag{11}$$

$$S_L = \left(B_m + B_\phi (\phi - \phi_m)^2\right) \cdot \left(\frac{Tu}{T_{ref}}\right)^\alpha \left(\frac{\rho}{\rho_{ref}}\right)^\beta f(\text{Dilution}) \tag{12}$$

$$f(\text{Dilution}) = 1 - 0.75 C_{DE} \cdot \cdot \left(1 - (1 - 0.75 C_{DE} \text{Dilution})\right)^7 \tag{13}$$

$$S_T = C_{TFS} u' \left(1 - \frac{1}{1 + C_{FkG}\left(\frac{R_f}{L_i}\right)^2}\right) \tag{14}$$

The combustion rate can be modified using multipliers such as Speed Multiplier (CTFS), Taylor Length Scale Multiplier (CTLS), Flame Kernel Growth Multiplier (CFKG), and Dilution Effect Multiplier (CDE). Modifying these multipliers changes the calculated combustion rate by the program, allowing the user to calibrate the calculated heat release values and the rate of heat release. This modification affects the parameters of the engine's thermodynamic cycle.

2.4. NO_x creation model

The calculation of NO is based on the extended Zeldovich mechanism. k1, k2, and k3 are the rate constants used respectively to calculate the reaction rates in the three equations below:

Nitrogen oxidation rate:

$$O + N_2 = NO + N \tag{k1}$$

Nitrogen oxidation rate:

$$N + O_2 = NO + O \tag{k2}$$

Hydroxyl oxidation rate:

$$N + OH = NO + H \tag{k3}$$

$$k1 = F_1 \cdot 7.6 \cdot 10^{10} \cdot e^{-38000 A_1 / T_b} \tag{15}$$

$$k2 = F_2 \cdot 6.4 \cdot 10^{6} \cdot e^{-3150 A_2 / T_b} \tag{16}$$

$$k3 = F_3 \cdot 4.1 \cdot 10^{10} \tag{17}$$

Using the multipliers found in the above eq. (15)–(17), the NO_x formation model can be calibrated. However, the creators of the GT Power software recommend using the default multipliers stored in the Zeldovich model settings.

2.5. HC creation model

The creation of HC during combustion is based on a simple quenching model on two plates with a simple kinetic model after flame extinction. A portion of the fuel-air mixture is pushed into the gap and trapped there during compression. During the expansion process, the trapped mixture begins to re-enter the main cylinder volume. Any mixture that re-enters the interior before the flame is extinguished will be burned according to the combustion model. The following kinetic reaction equation shows how the GT-Power solver calculates the HC value according to the SIturb combustion model.

$$R_k = 2000 \cdot AR_S [Fuel][O_2] e^{-1600K \cdot B/T} \tag{18}$$

2.6. CO creation model

The calculation of CO is based on the following mechanism and has been developed for homogeneous combustion:

$$CO + OH \rightleftharpoons CO_2 + HCO + OH \rightleftharpoons CO_2 + H$$

where K represents the equilibrium constant – equation (19)

$$K = 6.76 \cdot 10^7 A e^{T/1102B} \tag{19}$$

2.7. CO_2 and H_2O creation model

The GT Power program defaults to predicting 13 combustion products (N_2, O_2, CO_2, CO, H_2O, H_2, H, O, OH, NO, N, SO_2 if sulfur is present in the fuel). The above models describe the kinetics of NO_x, HC, and CO formation, while H_2O and CO_2 are the main products of hydrocarbon

combustion processes and are automatically included. Their mass concentrations in the exhaust gases are calculated by the solver based on the air-fuel ratio (AFR) ratio.

2.8. Injection and evaporation model

In the simulation, the model used is called InjPulseConn, which is a sequential injector model with a predefined pulse width. This model is used for simulating injection in direct injection (DI) engines. To define the injected liquid mass, two out of three parameters need to be defined: Injector Delivery Rate, Injection Pulse Width, or Injected Mass. The model also requires specifying the injection timing expressed in CAD (crank angle degrees), defining the diameter of the nozzle hole, the number of nozzles, and the flow loss coefficient, as well as defining the liquid injection model considering evaporation. The spray model takes into account various physical processes related to the evaporation of directly injected fuel. It models the penetration of the sprayed liquid, breakup of the liquid into droplets, entrainment of air and residual gases into the sprayed liquid, and droplet vaporization rate. Because this model is sensitive to various physical input data, it is important to have accurate information regarding the injection profile, nozzle hole diameter, flow coefficient, and fuel temperature.

2.9. Heat transfer model

The heat transfer model used in the simulation for the exchange of heat between the cylinder charge and the metal walls inside the cylinder is the Woschni model with consideration of the k-ε turbulence model. The Woschni model is based on Newton's equation for heat transfer, where the heat transfer coefficient is described by the equation (20):

$$h_C = \frac{K_1 P^{0.8} w^{0.8}}{B^{0.2} T^{K_2}} \tag{20}$$

3. Simulation set-up and boundary conditions

In this section, the initial conditions of the simulation, along with the settings, are presented in a tabular form. As mentioned above, the Honda engine is equipped with a carburetor fuel system. For the purpose of the simulation, the carburetor was modeled as an injector component, and the InjAF-RatioConn type was selected from the GT Power program base, which adjusts the delivered fuel mass based on the user-defined Air-Fuel Ratio (AFR) value. The simulations were divided into two main parts: simulation of engine operation without water injection into the cylinder and repeated simulations with the same settings and boundary conditions but with the inclusion of the water injection model into the cylinder. To achieve the most realistic representation of the water injection process, the injector characteristic was prepared and presented in Fig. 6. To best replicate the engine cycle, the model was calibrated against real indicated pressure measurements. The GT program contains a built-in module for optimizing selected parameters to most faithfully reproduce simulation results compared to experimental data. In this study, the model was optimized against three in-cylinder pressure measurements conducted for another research [10]. The sought-after optimization parameters aimed at the best calibration of simulation results were selected as multipliers of the equation describing the combustion rate according to the SITurb model, as well as lambda values and volumetric coefficient.

Table 2. Initial conditions for intake and exhaust systems

	T [K]	P [bar]
Intake system	300	1
Exhaust system	600	1.1

The combustion model setting used for the simulations are the following:

- Combustion model: **SI Turbulent Flame Combustion Model**
- Laminar flame speed: **standard for gasoline**
- Ignition timing advance angle: **27 deg bTDC const.**
- NO_x model: **Extended Zeldovich mechanism**
- Combustion model equation parameters: **Closed Volume Calibration values**
- Engine supply: **Model InjAF**
- Fuel model: **Indolene combustion**

Heat Transfer model is defined by the following settings:

- Heat exchange model: GT **Woschni**
- Overall Convection Multiplier: **1.1**
- Head/Bore Area Ratio: **1.3**
- Piston/Bore Area ratio: **1.03**
- Convection Temperature Evaluation: **On**

Cranktrain kinematic parameters are following:

- Cylinder bore x piston stroke **68 × 45 mm**
- Connecting rod length **84 mm**
- Compression ratio **8.5:1**

Water injection model settings are defined as:

- Water injection model: **InjPulseConn**
- Injection pressure: **50 bar**
- Nozzle hole diameter: **0.3 mm**
- Number of holes: **6**
- Flow loss coefficient: **0.7 (default)**
- Evaporation model: **EngCylSprayEvap**

The simulation scenarios with water injection are presented in Table 3.

Table 3. Simulation study scenario of water injection into the cylinder

n [rpm]	W/F	Injection timing CAD relative to TDC							
2000	0.1	–100	–80	–60	–40	–25	0	20	30
	0.15	–100	–80	–60	–40	–25	0	20	30
	0.2	–100	–80	–60	–40	–25	0	20	30
2500	0.1	–100	–80	–60	–40	–25	0	20	30
	0.15	–100	–80	–60	–40	–25	0	20	30
	0.2	–100	–80	–60	–40	–25	0	20	30
3000	0.1	–100	–80	–60	–40	–25	0	20	30
	0.15	–100	–80	–60	–40	–25	0	20	30
	0.2	–100	–80	–60	–40	–25	0	20	30

The injection timing and current injector flow rate depend, among other factors, on the pressure difference between the injected water and the current pressure in the cylinder. Table 3 shows that the simulated injection will occur at different crankshaft rotation angle values and, hence, at different cylinder pressures. To achieve the same W/F ratio value, the injection timing during the simulation will be calculated according to the following formula parameter.

$$t = \frac{m_f W/F}{C_d\sqrt{(2(P_{inj}-P_{cyl})/\rho_w}} NA_{nozzle}\rho_w \quad (21)$$

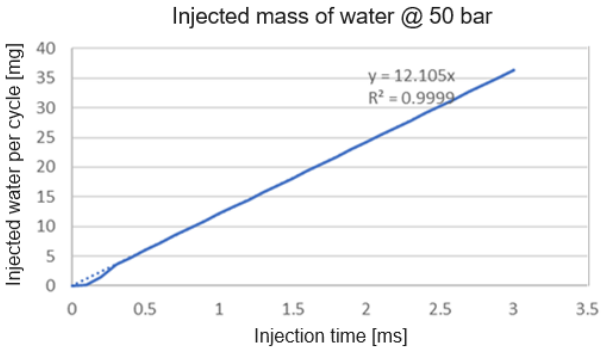

Fig. 6. Mass of injected water in a function of injection time

4. Results

4.1. Model calibration results

The computational model built above, along with the initial conditions, underwent optimization. An evolutionary algorithm with parameters as in Table 4 was used for this purpose. The aim was to achieve the most accurate fitting of the calculated cylinder pressure curve to the pressure curve measured for the research presented in the paper [10], where the engine ran at constant rotational speed and under a constant load provided by a 48 V 3-phase AC generator. The parameters sought were the multipliers of the equation describing the combustion rate according to the SITurbo Speed Multiplier (CTFS) model, Taylor Length Scale Multiplier (CTLS), Flame Kernel Growth Multiplier (CFKG), as well as the relative air-fuel ratio and volumetric efficiency. Below, a comparison of the actual measured indicated pressures for three engine speeds (Fig. 7–9) to the calculated pressure and values determined by the evolutionary optimization algorithm is shown.

Table 4. Genetic optimization parameters

Population size	30
Number of generations	34
Mutation rate	0.5

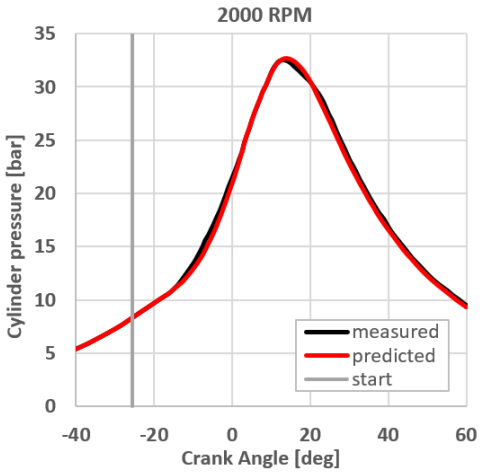

Fig. 7. A comparison between the calculated pressure, incorporating the constants determined during optimization, and the engine measured in-cylinder pressure at 2000 rpm

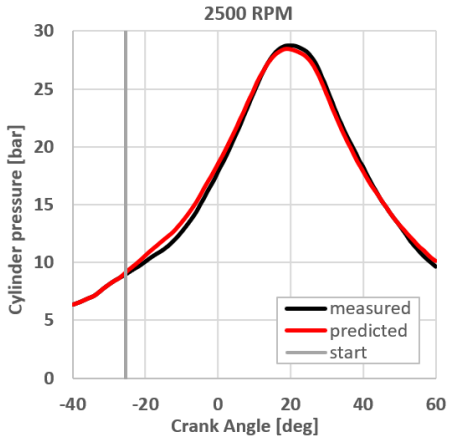

Fig. 8. A comparison between the calculated pressure, incorporating the constants determined during optimization, and the engine measured in-cylinder pressure at 2500 rpm

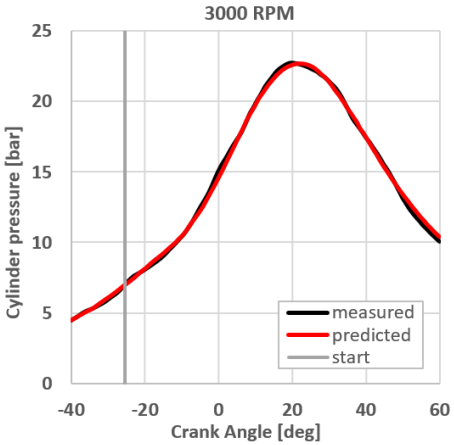

Fig. 9. A comparison between the calculated pressure, incorporating the constants determined during optimization, and the engine measured in-cylinder pressure at 3000 rpm

The combustion model parameters of SITurb obtained during genetic optimization are presented in Table 5. After the optimization calculated in-cylinder pressure profiles closely matched the measured pressures.

Table 5. The combustion model parameters of SITurb obtained during genetic optimization

Engine speed, rpm	2000	2500	3000
Dilution exponent multiplier	0.292934	0.323	0.331981
Flame kernel growth multiplier	2.443412	2.760911	2.875282
Turbulent flame speed multiplier	0.6934	0.560654	0.412272
Taylor length scale multiplier	2.30324	1.9888702	1.683686

4.2. Results of simulations with water injection for engine performance

The simulation results present four selected engine performance parameters: torque, specific fuel consumption, overall efficiency, and mean effective pressure. The absolute differences for direct water injection are not significantly different from the results for the cycle without water injection. A decrease in parameters can be observed, but it is not substantial.

4.2.1. W/F 0.1 results for engine performance

The analysis of results for 2000 rpm (Fig. 10–13) shows that the largest decrease in parameter values occurs for water injection at 100 deg bTDC (see Table 3). However, for an angle of 25 deg bTDC, which is two degrees after the ignition angle, the parameter values are closest to those of the cycle without water injection. A similar trend is observed in the results for 2500 rpm. For 3000 rpm, the weakest results are presented for water injection at 30 deg aTDC, and the trend is notably different. It can be observed that for injection before TDC and at TDC, the values are aligned, while there is a significant decrease for injection after TDC. Interestingly, for 3000 rpm, the best results were obtained for a water injection angle of 100 deg bTDC, which is completely opposite to the results for 2000 and 2500 rpm. Generally, numerically the smallest differences in parameters occur at an engine speed of 2500 rpm.

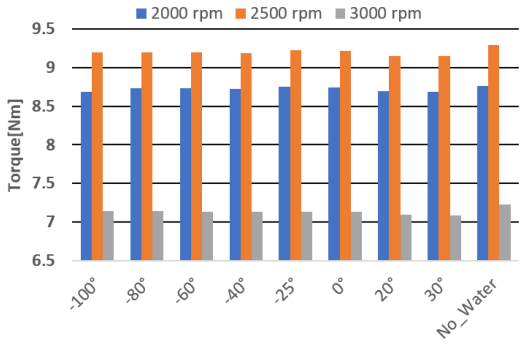

Fig. 10. Engine torque for the cycle without water injection and for each water injection angle for the W/F ratio of 0.1

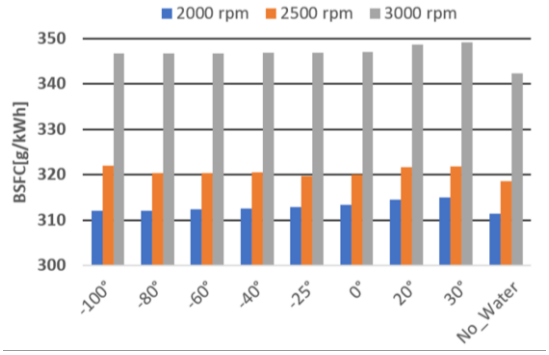

Fig. 11. Brake specific fuel consumption for the cycle without water injection and for each water injection angle for the W/F ratio of 0.1

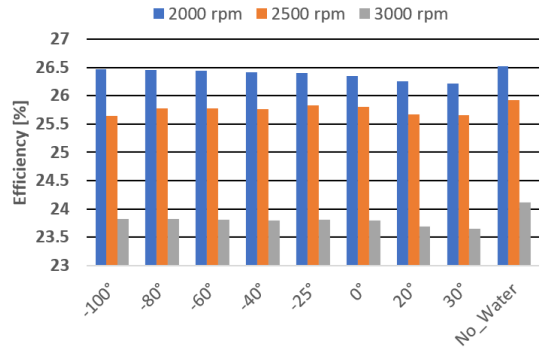

Fig. 12. Brake efficiency for the cycle without water injection and for each water injection angle for the W/F ratio of 0.1

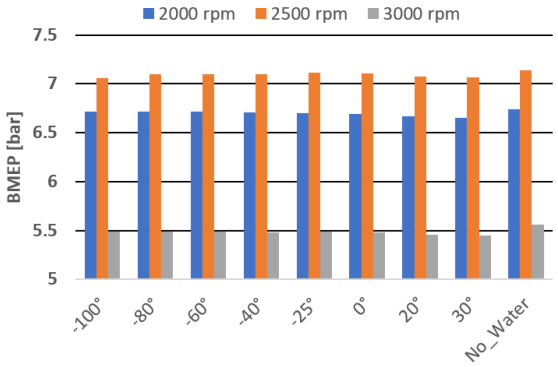

Fig. 13. Brake mean effective pressure for the cycle without water injection and for each water injection angle for the W/F ratio of 0.1

4.2.2. W/F 0.15 results for engine performance

For a water injection mass equal to 15% of the supplied fuel mass, simulation results show (Fig. 14–17) the best performance for water injection at 100 deg bTDC. The parameters are very close, as shown in the figures below. It is worth mentioning that for an engine speed of 2000 rpm, the difference in efficiency is 0.04%. As the injection angle increases relative to TDC, the parameters deteriorate approximately exponentially compared to the cycle without water injection, but the differences are very small and practically negligible from an engineering standpoint. For 2500 rpm, similar to the W/F ratio of 0.1, the smallest parameter losses occur for an injection angle equal to 25 deg bTDC. However, unlike the W/F ratio of 0.1, where for 2500 rpm the largest difference in parameters was for an injection angle of 100 deg bTDC, for the case of W/F ratio of 0.15, the weakest parameters are for an injection angle of 20 deg aTDC. On the other hand, for early injection angles, the parameters are very close. There are also greater differences in efficiency. Specifically, the efficiency compared to the cycle without water injection is an order of magnitude lower for each water injection, yet the differences are still very small. For an engine speed of 3000 rpm, the trend is similar to that of 2000 rpm, with the difference that for a value of 40 deg bTDC, a clear deviation from the trend of decreasing parameter values is observed. In this case, the parameters are minimally larger for 40 deg bTDC than for 25 deg bTDC and TDC. The best parameters are achieved for an injection at 100 deg bTDC. However, as observed, the losses for a speed of 3000 rpm are greater than for speeds of 2000 and 2500 rpm.

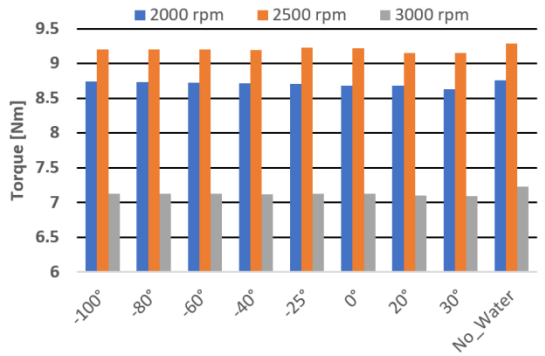

Fig. 14. Engine torque for the cycle without water injection and for each water injection angle for the W/F ratio of 0.15

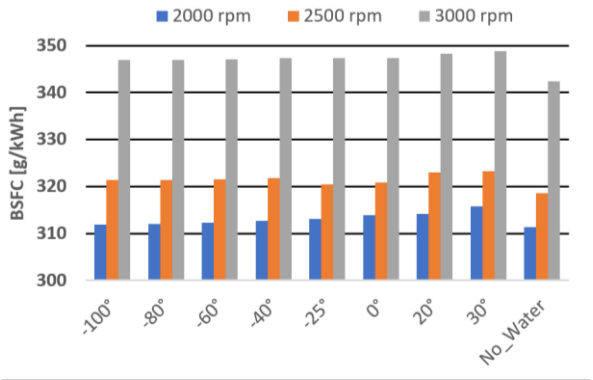

Fig. 15. Brake specific fuel consumption for the cycle without water injection and for each water injection angle for the W/F ratio of 0.15

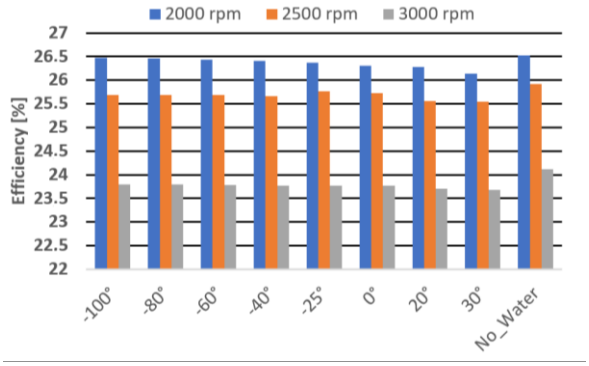

Fig. 16. Brake Efficiency for the cycle without water injection and for each water injection angle for the W/F ratio of 0.15

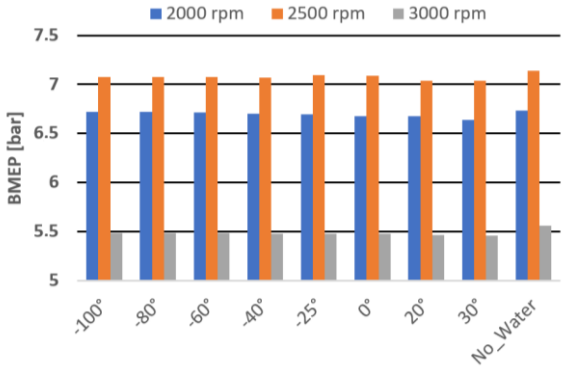

Fig. 17. Brake mean effective pressure for the cycle without water injection and for each water injection angle for the W/F ratio of 0.15

4.2.3. W/F 0.2 results for engine performance

For a water injection mass equal to 20% of the supplied fuel mass, similar to the W/F ratios of 0.1 and 0.15, the losses in torque, specific fuel consumption, overall efficiency, and mean effective pressure are very small (Fig. 18–21). However, compared to the previously discussed results for the W/F ratio of 0.2, these losses are numerically the smallest. The trend for 2000 rpm is similar to that of the W/F ratio of 0.15; however, the losses are slightly smaller. The overall efficiency for this case is closest to the efficiency of the cycle without water injection among all simulated points and is only 2.6% lower. Similarly, the simulation shows that the best solution is water injection at 100 deg bTDC, while the worst results are for water injection at 20 deg aTDC. For an engine speed of 2500 rpm, the best results, as with the two earlier W/F ratios, are obtained for water injection at 25 deg bTDC, while the worst results are obtained for late injection at 30 deg aTDC. At an engine speed of 3000 rpm, as in the previous considerations, the results for the injection angle range between 100 bTDC and TDC are very close, with a clear deviation for 40 deg bTDC. However, unlike the previous results for a smaller amount of injected water, in this case, the best results are obtained for water injection at 80 deg bTDC, although the difference between the remaining results is negligible. The weakest results are for late water injection angles after TDC.

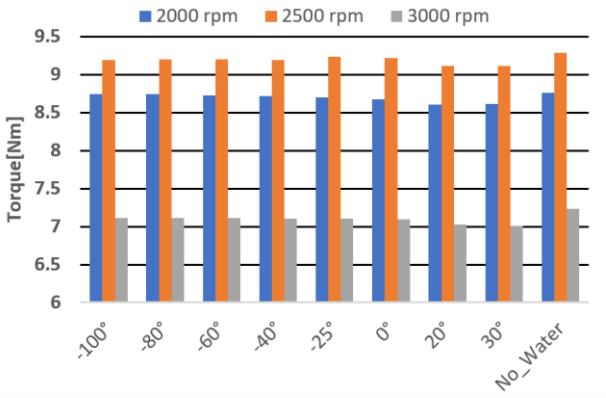

Fig. 18. Engine torque for the cycle without water injection and for each water injection angle for the W/F ratio of 0.2

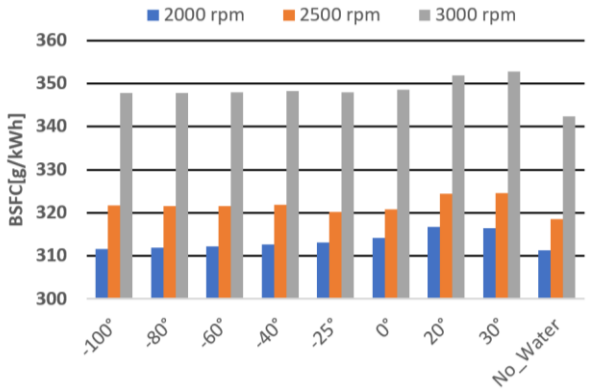

Fig. 19. Brake specific fuel consumption for the cycle without water injection and for each water injection angle for the W/F ratio of 0.2

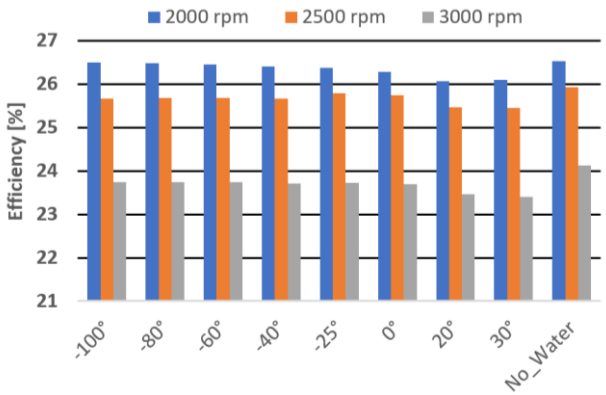

Fig. 20. Brake efficiency for the cycle without water injection and for each water injection angle for the W/F ratio of 0.2

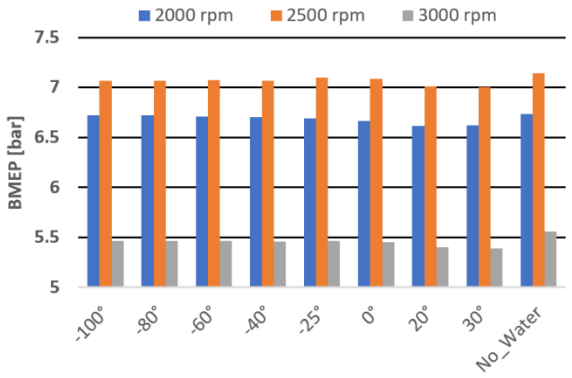

Fig. 21. Brake mean effective pressure for the cycle without water injection and for each water injection angle for the W/F ratio of 0.2

4.3. Results of simulations with water injection for exhaust gas concentration

The results indicate a clear reduction in NO_x and CO_2 emissions for some cases, with a decrease also observed in CO emissions, while an increase in HC emissions is noticeable. A detailed presentation of emission results for simulations for each W/F ratio is provided in the following subsections.

4.3.1. W/F 0.1 results for exhaust gases concentration

For 2000 rpm, at an injection angle of 100 deg bTDC, NO_x emissions decrease by 24%, while at an injection angle of 30 deg aTDC, they decrease by 7.5%. CO emissions, on the other hand, increased over fourfold for every water injection scenario. CO_2, meanwhile, decreased by approximately 1.4%. The lowest decrease in emissions was observed for an injection angle of 30 deg aTDC, with a decrease of 1.68%. However, the HC emissions for this same angle were the highest, increasing fifteenfold compared to the cycle without water injection. The lowest increase in HC emissions was obtained for injection at TDC, increasing by 5.28%. For 2000 rpm, the results show a decrease in NO_x, CO, CO_2 emissions, and an increase in HC emissions compared to the cycle without water injection. The lowest emissions of NO_x, CO, and CO_2 were observed for water injection at 100 deg bTDC, while HC emissions, similar to the engine speed of 2000 rpm, were highest for water injection at TDC, and for 2500 rpm, they were higher than the cycle without water addition by 5.6%. For late water injection after TDC, HC emissions increase by 51.6% for 20 deg aTDC and by 110.7% for 30 deg aTDC.

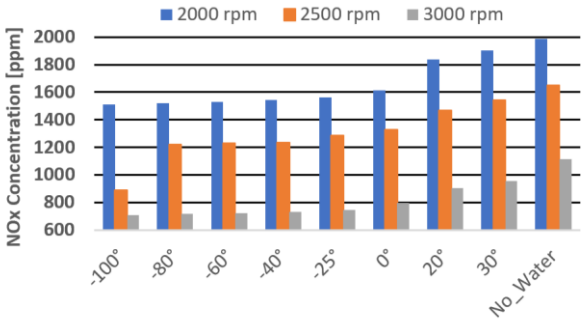

Fig. 22. NO_x concentration in ppm for the cycle without water injection and for each water injection angle for the W/F ratio of 0.1

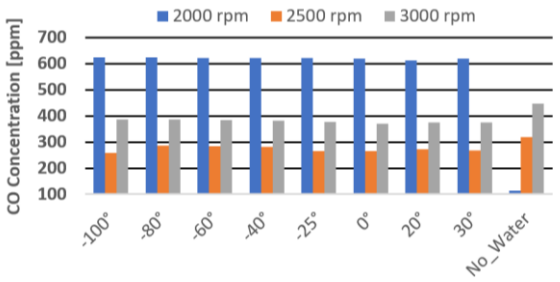

Fig. 23. CO concentration in ppm for the cycle without water injection and for each water injection angle for the W/F ratio of 0.1

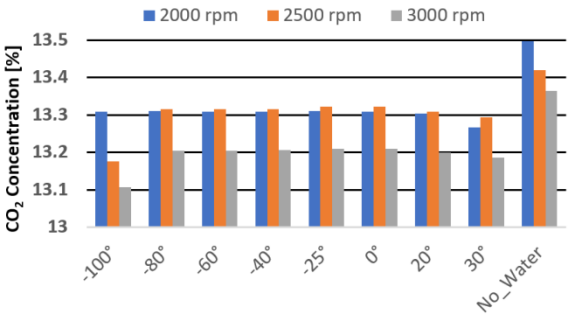

Fig. 24. CO_2 concentration for the cycle without water injection and for each water injection angle for the W/F ratio of 0.1

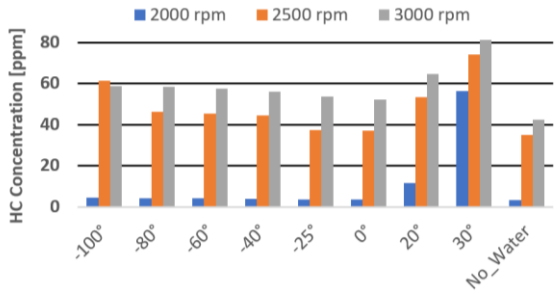

Fig. 25. HC concentration in ppm for the cycle without water injection and for each water injection angle for the W/F ratio of 0.1

4.3.2. W/F 0.15 exhaust gases concentration

The trend in reducing NO_x emissions at 2000 rpm looks similar to that for the W/F ratio of 0.1; however, the lowest emissions achieved for the same injection angle of 100 deg bTDC are 33.9% lower compared to the cycle without water addition. For CO_2 emissions, the situation is similar, with a decrease observed, but compared to the W/F ratio of 0.1, the decrease for 30 deg aTDC is at the level of 2.26%.

The situation with the increase in CO and HC emissions also appears similar, with a fourfold increase in CO emissions and a sharp rise in HC emissions for an injection angle of 30 deg aTDC, which in this case was 19 times higher than in the cycle without water injection. For engine speeds of 2500 and 3000 rpm, compared to 2000 rpm, there is a decrease in CO emissions, and the trend for both cases looks similar, but the emissions for 3000 rpm relative to the cycle without water injection appear slightly better than for 2500 rpm. Also, in these cases, there is a significant deterioration in HC emissions for late water injection angles after TDC, precisely for an angle of 30 deg aTDC, where HC concentrations are the highest, and their increase looks as follows: for 2500 rpm, an increase of 191.8%, while for 3000 rpm, it is more than two times lower, at 81.4%.

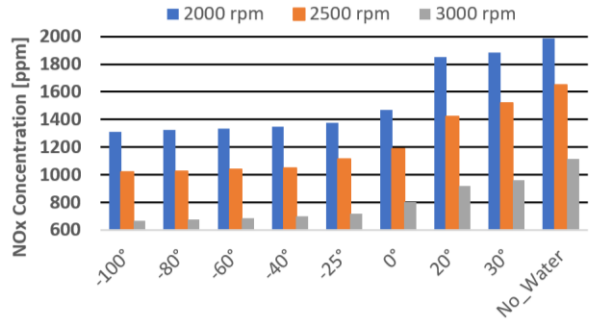

Fig. 26. NO_x concentration in ppm for the cycle without water injection and for each water injection angle for the W/F ratio of 0.15

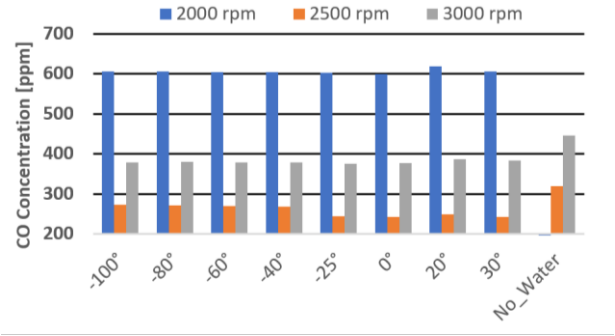

Fig. 27. CO concentration in ppm for the cycle without water injection and for each water injection angle for the W/F ratio of 0.15

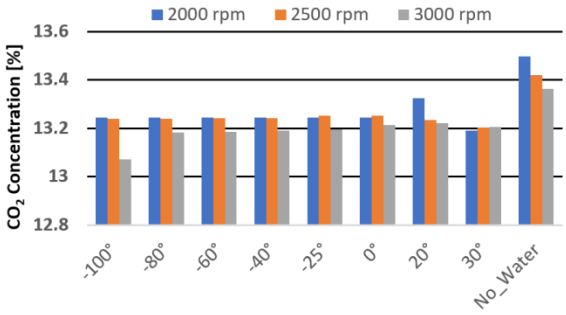

Fig. 28. CO_2 concentration for the cycle without water injection and for each water injection angle for the W/F ratio of 0.15

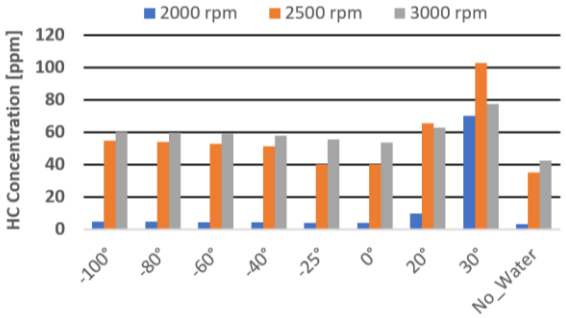

Fig. 29. HC concentration in ppm for the cycle without water injection and for each water injection angle for the W/F ratio of 0.15

4.3.3. W/F 0.2 results for exhaust gas concentration.

The results for concentration levels for the W/F ratio of 0.2 appear to be the most favorable compared to simulations with lower water addition amounts. For 2000 rpm, the trend is the same as for lower water additions, with the difference being that the percentage reduction in NO_x and CO_2 emissions numerically is greater than for the two previous water additions, respectively. The smallest NO_x emissions for 100 deg bTDC are lower by 42.3% compared to the cycle without water injection, and the CO_2 emissions are lower by 2.8%. Similarly, CO and HC emissions increase, but numerically, the increase in CO emissions looks better because its increment is slightly smaller than fourfold compared to CO emissions without water addition. Interestingly, the maximum increase in HC emissions for 30 deg aTDC is as much as 22 times higher. Similarly, for 2500 and 3000 rpm, emissions appear better except for HC emissions, which are higher than for cases where the W/F ratio was 0.1 and 0.15, respectively. The greatest reduction in NO_x, CO, and CO_2 was achieved in the simulation for 3000 rpm.

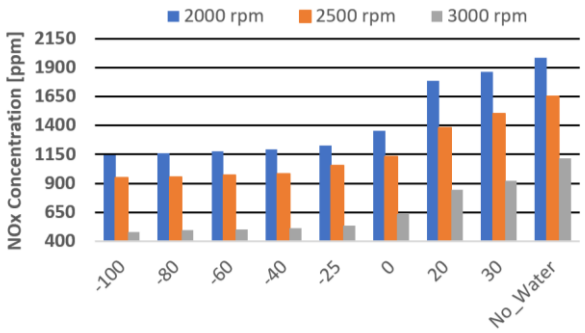

Fig. 30. NO_x concentration in ppm for the cycle without water injection and for each water injection angle for the W/F ratio of 0.2

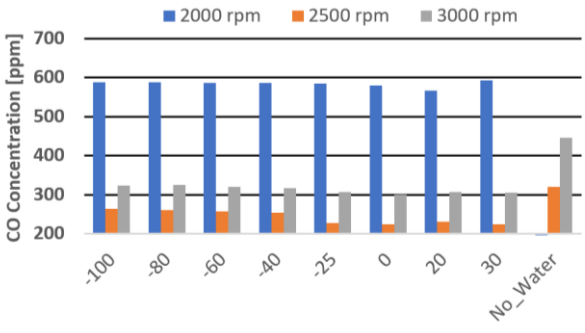

Fig. 31. CO concentration in ppm for the cycle without water injection and for each water injection angle for the W/F ratio of 0.2

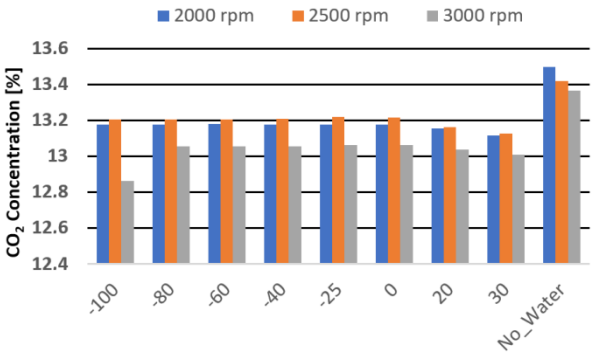

Fig. 32. CO_2 concentration for the cycle without water injection and for each water injection angle for the W/F ratio of 0.2

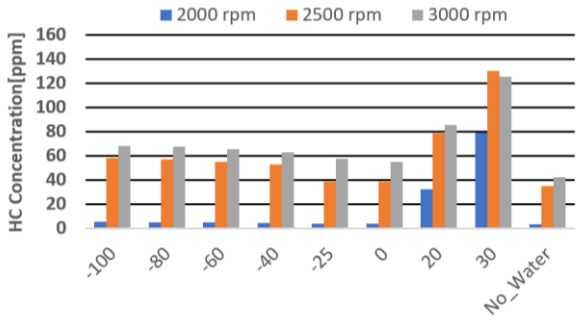

Fig. 33. HC concentration in ppm for the cycle without water injection and for each water injection angle for the W/F ratio of 0.2

5. Results discussion and conclusions

The simulation results showed that direct water injection slightly deteriorates the performance of the analyzed engine. The maximum difference in torque compared to cycles without water injection is less than 0.25 Nm. The indicated pressure, which is related to torque, also does not differ much from the comparative pressure calculated by the program for cycles without water addition and is less than 0.2 bar. The overall efficiency, with the highest calculated decrease being less than 0.9%, and the specific fuel consumption is higher, in the worst case, by less than 10.5 g/kWh.

Regarding the injection angle, two distinct values can be distinguished for which the parameters are closest to the cycle without water addition: 25 deg bTDC and 100 deg bTDC. Depending on the W/F ratio and engine speed, for 2000, 2500, and 3000 rpm, the best values for the W/F ratio of 0.1 were achieved at injection angles of –25, 100, and 100 deg bTDC, respectively. For the W/F ratio of 0.15, the relationship was reversed, with angles of –25, 100, and 100 deg bTDC, respectively. However, for the W/F ratio of 0.2, the best results were achieved at angles of 25, 100, and 80 deg bTDC, respectively. For 3000 rpm, where the best angle was found to be 80 deg bTDC, the difference in results compared to an angle of 100 deg bTDC is of the order of ten thousandths.

However, it is evident that injection during the final phase of combustion, although the results are also close to those of the cycle without water injection, performed worse compared to injection angles before TDC.

The general conclusion regarding the impact of direct water injection into the SI engine cylinder based on simulation results is that water injection should not significantly decrease engine performance parameters. However, a significant improvement in emission levels can be observed, especially in the reduction of NO_x emissions, which is consistent with expectations due to the decrease in the average cycle temperature. For all analyzed scenarios, the greatest reduction in NO_x emissions occurred at an injection angle of 100 deg bTDC, with the highest reduction of 56.8% achieved for the W/F ratio of 0.2 at an engine speed of 3000 rpm. Similarly, CO_2 emissions were lower for all considered scenarios. The largest reduction in CO_2 emissions also occurred for an engine speed of 3000 rpm, a W/F ratio of 0.2, and an injection angle of 100 deg bTDC, with a decrease of 3.75%.

Regarding the impact of injection strategy on CO_2 emissions, two values can be distinguished, in addition to the previously mentioned injection angle of 100 deg bTDC, for which the lowest emissions were achieved at engine speeds of 2500 and 3000 rpm for the W/F ratio of 0.1 and at 3000 rpm for the W/F ratios of 0.15 and 0.2. Additionally, injection at 30 deg aTDC, during the end of the combustion process, resulted in the greatest reduction in CO_2 emissions at 2000 rpm for the W/F ratio of 0.1, 2000 and 2500 rpm for the W/F ratio of 0.15 and 0.2. CO emissions also decreased, except for the scenario with an engine speed of 2000 rpm, where the increase in CO emissions, depending on the water injection angle, oscillated between four and four and a half times higher than in the case without water injection. For other engine speeds, the simulation showed a decrease in CO emissions, with the greatest reduction achieved for an engine speed of 3000 rpm and a W/F ratio of 0.2 at an injection angle of TDC. For an injection angle of TDC, in most cases, the lowest CO emissions were obtained, except for an engine speed of 3000 rpm and a W/F ratio of 0.15, where the lowest emissions were obtained at 25 deg bTDC, and for an engine speed of 2500 rpm and a W/F ratio of 0.1, where the lowest emissions were obtained at 100 deg bTDC. However, the simulations showed an increase in HC emissions for all cases, especially for an injection angle of 30 deg aTDC. The worst-case scenario was at 2000 rpm for the W/F ratio of 0.2, where the HC emission level was as much as 22 times higher compared to the cycle without water injection. Similarly large increases in HC emissions were observed for a water injection angle of 20 deg aTDC, indicating that late water injection during the final combustion phase increases HC emissions. The smallest increase in HC emissions was obtained for all cases for water injection at TDC, with the lowest increase for this water injection angle obtained for an engine speed of 2000 rpm at a W/F ratio of 0.1. Thus, it can be concluded that an increase in water mass in the cylinder increases HC emissions, while the same increase in water mass reduces NO_x, CO_2, and CO emissions.

It is also important to note that the reduction in the average cycle temperature and the decrease in the thermal energy flux transferred to the engine's metallic components also increase the engine's lifespan by reducing thermomechanical loads. However, direct water injection can also cause dilution of the engine lubricating oil, unevaporated water can deposit on the cylinder walls, and mix with the oil, worsening its lubricating properties.

It should also be noted that the results discussed above are the outcomes of one-dimensional mathematical-physical models' simulations and may be subject to error. The accuracy of the simulations can only be assessed through physical tests with a replicated scenario, which would allow for the validation of the numerical model. Further steps in the research work will involve setting up a test bench and conducting experiments, which will unequivocally confirm the simulation results.

Acknowledgements

The GT-Power license used for calculations in this publication was provided by Jenbacher Polska sp. z o.o., where Mr. Konrad Kuchmacz is employed. The authors would like to thank the company for its assistance, without which the preparation of this article would not have been possible.

Nomenclature

A	pre-exponent multiplier
A	cross-sectional flow area
A_1	N_2 oxidation activation energy multiplier
A_2	N oxidation activation energy multiplier
Ae	surface area at flame front
A_{eff}	effective flow area
A_R	reference flow area
A_s	heat transfer surface area
aTDC	after top dead center
B	activation temperature multiplier
B	cylinder bore diameter
Bm	maximum laminar speed
BΦ	laminar speed roll off value
bTDC	before top dead center
C_D	discharge coefficient
C_f	fanning friction factor
D	equivalent diameter
D	valve diameter
DWI	direct water injection
dp	pressure differential acting across dx
d_x	length of mass element in the flow direction (discretization length)
e	total specific internal energy (internal energy plus kinetic energy per unit mass)
F_1	N_2 oxidation rate multiplier
F_2	N oxidation rate multiplier
F_3	OH reduction rate multiplier
[Fuel]	mass fraction of fuel
H	Total specific enthalpy,
h_c	heat transfer coefficient
K_1, K_2	equation constant equal 3.26 and 0.53
K_p	pressure loss coefficient (commonly due to bend, taper or restriction)
L	valve lift
Li	integral length scale
M	mass of the volume
Mb	burned mass
Me	entrained mass
$[O_2]$	mass fraction of oxygen
p	pressure
P	in-cylinder pressure
P_R	absolute pressure ratio (static pressure at the throat/total inlet pressure)
pref	101325 Pa
R	gas constant
Ret	turbulent Reynolds number
Rf	flame radius
Rk	kinetic burn rate (mass per volume per sec)
Rs	SITurb burn rate (mass per volume per sec)
SL	laminar flame speed dilution residual mass fraction in unburned zone
ST	turbulent flame speed
t	time
T	cylinder temperature
T	mass averaged overall cylinder temperature (K)
T_b	burned subzone temperature (K)
T_{fluid}	fluid temperature
T_o	upstream stagnation temperature
TDC	top dead center
Tref	298 K
Tu	unburned gas temperature
T_{wall}	wall temperature
U	velocity at the boundary
u'	turbulent intensity
U_{is}	isentropic velocity at the throat
V	volume
W/F	water to fuel ratio
w	gas velocity
α	temperature exponent
β	pressure exponent
γ	specific heat ratio (1.4 for air at 300 K)
λ	Taylor microscale length
ρ	density
ρ_{is}	density at the throat
ρ_o	upstream stagnation density
ρu	unburned density
Φ	equivalence ratio
Φm	equivalence ratio at maximum speed
$\dot{m}$	boundary mass flux into volume
$\dot{m}$	mass flow rate

Bibliography

[1] Berni F, Breda S, Lugli M, Cantore G. A numerical investigation on the potentials of water injection to increase knock resistance and reduce fuel consumption in highly downsized GDI engines. Enrgy Proced. 2015;81:826-835. https://doi.org/10.1016/j.egypro.2015.12.091

[2] Cantani A, Viggiano A, Magi A. On direct injection of supercritical water into spark ignition engines as a strategy for heat recovery. Energy Technology, 2021;9:2100198. https://doi.org/10.1002/ente.202100198

[3] Chen H, Wang C, Li X, Li Y, Zhang M, Peng Z et al. Quantitative analysis of water injection mass and timing effects on oxy-fuel combustion characteristics in a GDI engine fuelled with E10. Sustainability. 2023;15:10290. https://doi.org/10.3390/su151310290

[4] Falfari S, Bianchi G, Cazzoli G, Forte C, Negro S. Basics on water injection process for gasoline engines. Enrgy Proced. 2018;148:50-57. https://doi.org/10.1016/j.egypro.2018.08.018.

[5] Ghazal OH, Borowski G. Use of water injection technique to improve the combustion efficiency of the spark-ignition engine: a model study. Journal of Ecological Engineering. 2019; 20(2):226-233. https://doi.org/10.12911/22998993/99689

[6] Li A, Zheng Z, Song Y. A simulation study of water injection position and pressure on the knock, combustion, and emissions of a direct injection gasoline engine. ACS Omega. 2021; 6(28):18033-18053. https://doi.org/10.1021/acsomega.1c01792

[7] Li X, Pei Y, Li D, Ajmal T, Rana KJ, Aitouche A et al. Effects of water injection strategies on oxy-fuel combustion characteristics of a dual-injection spark ignition engine. Energies. 2021;14:5287. https://doi.org/10.3390/en14175287

[8] Millo F, Gullino G, Rolando L. Methodological approach for 1D simulation of port water injection for knock mitigation in a turbocharged DISI engine. Energies. 2020;13:4297. https://doi.org/10.3390/en13174297

[9] Mishra S, Naik B, Mallikarjuna JM. Effect of direct water injection timing and quantity on combustion, performance, and emission characteristics of a homogeneous charge compression ignition engine − a CFD analysis. Appl Therm Eng. 2024;257B:124190. https://doi.org/10.1016/j.applthermaleng.2024.124190

[10] Noga M, Moskal T. Evaluation of a pressure sensing glow plug in terms of its application possibility to control the combustion process of a hydrogen-powered spark-ignition engine. Combustion Engines. 2024;196(1):140-145. https://doi.org/10.19206/CE-172820

[11] Pryciński P, Pielecha P, Korzeb J, Pielecha, J, Kostrzewski M, Eliwa A. Air pollutant emissions of passenger cars in Poland in terms of their environmental impact and type of energy consumption. Energies. 2024;17 :5357. https://doi.org/10.3390/en17215357

[12] Stępień Z. Vehicle related non exhaust particle emissions – Euro 7 requirements. Combustion Engines. 2024;199(4):15-29. https://doi.org/10.19206/CE-190606

[13] Voris AR, Lundberg M, Puzinauskas PV. Effect of ethanol content, water injection, and compression ratio on combustion and detailed emissions in an SI-GDI engine. Fuel. 2025;381A: 133200. https://doi.org/10.1016/j.fuel.2024.133200

[14] Zhang Z, Dai X, Zheng Z, Numerical simulation study on the effect of port water injector position on the gasoline direct injection engine. Processes. 2022;10:1909. https://doi.org/10.3390/pr10101909

[15] Zhuang Y, Lin Z, Zhai R, Huang Y, Nie B, Li Y. A study on the effect of spark plug micro-hole hydrogen injection on the spray and combustion processes of a gasoline engine with intake port water injection. Energy. 2025;315:134366. https://doi.org/10.1016/j.energy.2025.134366

[16] GT Power 2019 Documentation. User Guide-Fluid Theory. 2019.

[17] The new BMW M4 GTS. https://www.press.bmwgroup.com/global/article/detail/T0236962EN/the-new-bmw-m4-gts

Konrad Kuchmacz, MEng. – Faculty of Mechanical Engineering, Cracow University of Technology, Poland.
e-mail: *konrad.kuchmacz@doktorant.pk.edu.pl*

Marcin Noga, DSc., DEng. – Faculty of Mechanical Engineering, Cracow University of Technology, Poland.
e-mail: *marcin.noga@pk.edu.pl*